Stabilization of Poly(dA)·[poly(dT)]$_2$ Triple Helical DNA by Acridine Derivatives: Role of Side Chain in the Triplex Stabilization

Kyung-Mee Hyun, Gil-Jun Lee, Tae-Sub Cho, Seog K. Kim*, and Seh Yoon Yi†

Department of Chemistry, Yeungnam University, Kyoungsan, Kyoung-buk 712-749, Korea
†Department of Chemistry, Ewha Womans University, Seoul 120-750, Korea
Received March 3, 1997

The conformation and stabilization effects of acridine derivatives 9-aminoacridine, an acridine with an aminoalkyl side chain, bis acridine (two acridines linked by an aminoalkyl side chain), and proflavin in the triplex helical poly(dA)·[poly(dT)]$_2$ were investigated by optical spectroscopies. Based on the negative LD and weak positive CD in the acridine absorption wavelength region, we concluded that the acridine moiety of all derivatives are intercalated. We also examined the melting temperatures. Of all the compounds examined, the acridine with an amino alkyl side chain had the strongest effect on the stabilization of the third strand of a poly (dA)·[poly(dT)]$_2$ triplex. The role of the side chain, based on this observation, is discussed.

Introduction

Interests in triple helical DNA increased following the discovery that short oligonucleotides can recognize specific sequences of duplex DNA[1-3] and that intramolecular triple helical DNA (H-DNA) can be formed in natural DNA.[4-7] Subsequent studies focused on both biological and therapeutic applications,[8] such as inhibiting the transcription[9-13] or replication[14,15] of specific sequences, and preventing cellular proteins from binding to their designated target DNA,[16-18] as well as on the design of artificial sequence specific nucleases.[19-21] The third strand generally binds less strongly to the duplex in physiological conditions than the two Watson-Crick base-paired strands of the corresponding duplex. Several attempts have been made to enhance the stability of the third strand, including using photoactivated cross linking reagents,[22,23] attaching intercalators to the third strand oligonucleotides,[24] and use of the triplex selective intercalators such as benzopyridoindoles (BePI).[25-29] All of these methods suggest the importance of the ligand-DNA interaction.

Several duplex binding ligands, such as intercalators, minor groove binders, and major groove binders, have been reported to interact with the triple helical DNAs. Ethidium bromide,[30,31] benzo[e]pyridoindole (BePI),[25-29] and 9-aminoacridine[32] and their derivatives, which are intercalators for duplex DNA, have been reported to intercalate between the base triplets and to stabilize the third strand. An interaction between minor groove binding ligands and triple helical DNA was also reported. Distamycin, which is known to bind highly selectively to the minor groove of B-form DNA but not to A-form DNA, binds to the poly(dA)·[poly(dT)]$_2$ triplex,[33,34] suggesting that vicinity of the distamycin binding site of the triplex adopts a B-form conformation. The binding of netropsin and berenil to the intramolecular triplex (dA)$_{12}$-x-(dT)$_{12}$-x-(dT)$_{12}$ (where x is a hexaethylene glycol chain) was studied by CD and thermal denaturation,[35,36] which revealed that the duplex- and triplex-bound ligands possess a similar conformation. A similarity in the conformation of duplex- and triplex- bound minor groove binding ligands was also confirmed for 4',6-diamidino-2-phenylindole (DAPI) and Hoechst 33258.[34] Minor groove binders generally do not affect or destabilize the third strand, despite the fact that they strongly stabilize corresponding duplexes (except for berenil, which stabilizes the third strand when NaCl is not present). Ligands which bind to the major groove of the duplex (methyl green[37]) or intercalates (methylene blue[38]) did not bind to the triplex.

Intercalators generally enhance the thermal stability of the third strand. To examine the triplex stabilization mechanism used by intercalators, we investigated the interaction of one intercalator, 9-aminoacridine (9AA), and three related derivatives (Figure 1) with a poly(dA)·[poly(dT)]$_2$ triplex. The two main questions we address in this study are (1) whether the side-chain changes the stabilization of the triplex (for this purposes, we included 9AA-pro, which has an aminoalkyl side chain, and bis-9AA, which is a bis-intercalator with a side chain) and (2) how the amine group at position 9 affect the stability of the third strand. Proflavine was included because the amine group at the position 9 of 9AA is replaced by amine groups at the position 3 and 6, enabling us to observe the role of the amine group.

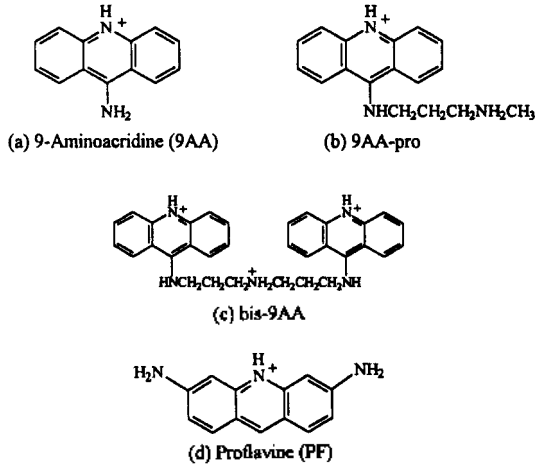

Figure 1. Molecular structures of 9AA, 9AA-pro, bis-9AA and proflavine.

Experiment

Materials. Polynucleotides were purchased from Pharmacia. 9AA and other derivatives from Sigma. 9AA-Pro and bis-9AA were gifts form Professor Ole Buchardt of Copenhagen University. Throughout this work, a 5 mM cacodylate buffer at pH 7.0 containing 1 mM (for the conformational study) or 100 μM $MgCl_2$ (for the melting profiles) were used. The concentrations of chemicals and polynucleotide were determined by the following molar extinction coefficients: $\varepsilon_{257\,nm}$=8,600 $M^{-1}cm^{-1}$ for poly(dA), $\varepsilon_{264\,nm}$=8,520 $M^{-1}cm^{-1}$ for poly(dT), $\varepsilon_{400\,nm}$=9,300 $M^{-1}cm^{-1}$ for 9-AA and 9AA-Pro, $\varepsilon_{406\,nm}$=18,000 $M^{-1}cm^{-1}$ for bis-9AA, $\varepsilon_{444\,nm}$=43,000 $M^{-1}cm^{-1}$ for proflavine.

The poly(dA)·[poly(dT)]$_2$ triplex was prepared by incubating a 1:2 molar ratio of poly(dA) and poly(dT) at 90 °C for 30 minutes, followed by overnight annealing at room temperature. The triplex formation was confirmed by its characteristic CD spectrum and biphasic melting profile. The concentration of poly(dA)·[poly(dT)]$_2$ triplex was fixed at 25 μM (in base triplet) with the mixing ratio ([ligands] per [base triplet]) of 0.10 for spectroscopic study and 14 μM for melting study. It should be noted that bis-9AA possess two acridine moiety per molecule, *i.e.*, a mixing ratio of 0.1 for the bis-9AA-poly(dA)·[poly(dT)]$_2$ triplex indicates 2 acridine chromophores per 10 base triplet.

Melting profiles. The dissociation of a polynucleotide strand from a double or triple helical polynucleotide manifests itself as a hyperchromism in the absorbance in the 260 nm region. The melting profiles were monitored by an HP 8452A diode array spectrophotometer equipped with an HP 80890A peltier temperature controller. The temperature was increased at a rate of 0.1 °C/min from 35 °C to 75 °C, with a reading taken every 2 minutes. We allowed sufficient time before the reading to ensure the equilibrium.

Circular dichroism (CD). CD is defined as the difference between the absorbances measured with left – and right hand circularly polarized light. Although all ligands in this study are achiral molecules, they acquire a CD signal when they bind to polynucleotides. This CD signal is thought to be induced by the interaction between the bound ligand and chirally arranged base transitions and to be dependent upon the position and orientation of the ligand with respect to the nucleo-bases.[39-41] All CD spectra were recorded on a Jasco J-720 spectropolarimeter using 1 cm path quartz cell. In some cases, the spectra were averaged over an appropriate number of scans.

LD and LD′. LD is defined as the differential absorption of the light polarized parallel and perpendicular to some laboratory reference axis; in the case of flow LD, the parallel direction is the flow direction.[41] The measured LD spectrum is then divided by the isotropic absorption spectrum to give the reduced linear dichroism spectrum(LD′). The magnitude of the LD′ spectrum depends on two factors, namely, S and O, the orientation and optical factors, respectively.[41-43]

$$LD'(\lambda)=S\times O=3S\,\frac{(<3\cos^2\alpha>-1)}{2}$$

The optical factor depends on the angel, α, that the transition moment of the ligand makes with the polynucleotide helix axis. The brackets denote the ensemble average over the angular distribution. The DNA bases have values close to 90°. Large ligand values (80-90°) are indicative of intercalation, whereas values ranging from 40° to 50° are consistent with the transition lying along the minor groove. The orientation factor, S, reflects the orientation degree of the polynucleotide in the flow; S would be unity for a polynucleotide perfectly aligned parallel to the flow direction and S=0 for an isotropic sample. If the DNA and ligand transition do not overlap, S is determined from the polynucleotide dichroism at 260 nm, assuming an effective angle of 86° between the $\pi\rightarrow\pi^*$ transition moments of the nucleotide bases and the polynucleotide helix axis.[41] The LD spectra of the flow-oriented sample were measured on a Jasco J-500C, equipped with an Oxley prism to convert the circularly polarized light into linearly polarized light.[42]

Result

Effect of the ligands on the stabilization of triplex poly(dA)·[poly(dT)]$_2$. Figure 2a and 2b show the effect of 9AA, bis-9AA, and 9AA-pro on the thermal stability of the poly(dA)·[poly(dT)]$_2$ triplex. The melting profile of the triplex was biphasic. The first melting (T_{m1}), which corresponds to the transition from the poly(dA)·[poly(dT)]$_2$ triplex to poly(dA)·poly(dT) plus poly(dT), occurred at 42.4 °C. The second melting (T_{m2}), corresponding to the dissociation of the poly(dA)·poly(dT) to poly(dA) and poly(dT), occurred at 65 °C. An independent melting study of poly(dA)·poly(dT) in the same solution indicated a melting temperature of 67 °C, confirming that the first melting for the triplex was the dissociation of the Hoogsteen-paired third strand. The first melting temperature reported in this study is quite low compared to a reported value in the same solution.[32] This difference may be related to the conditions of the stabilization in which the conformation of the triplex is known to be extremely sensitive. However, our present results are not affected by this point because our conditions were strictly maintained throughout this work. All three compounds, 9AA, 9AA-pro and bis-9AA, which all consist of intercalating moiety plus side chains, effectively stabilized the third strand of the poly(dA)·[poly(dT)]$_2$ triplex (Figure 2a). As the mixing ratio is increased, the thermal stability of the third strand was enhanced (Figure 2b). In the presence of 9AA or bis-9AA, the T_{m1} increases from 42.4 °C to ~49 °C at a mixing ratio of 0.1, which corresponds to 1 intercalated ligand per 10 base triplets for 9AA and 2 intercalated chromophores per 10 base triplets for bis-9AA (see below for intercalation). This indicates that 9AA is slightly more effective than bis-9AA in third strand stabilization. Surprisingly, 9AA-pro stabilized the third strand most effectively (Figure 2b). At a mixing ratio of 0.1, the T_{m1} reaches to ~60 °C.

The melting profile of the poly(dA)·[poly(dT)]$_2$ triplex in the presence of proflavine, which possesses different subsituents of acridine moiety, is almost the same as that of the triplex-9AA mixture (data not shown), suggesting that the stabilization effect of proflavin is similar to 9AA, even though the amine group at position 9 is exchanged with those at position 3 and 6.

Spectroscopic properties of the 9AA-pro and pro-

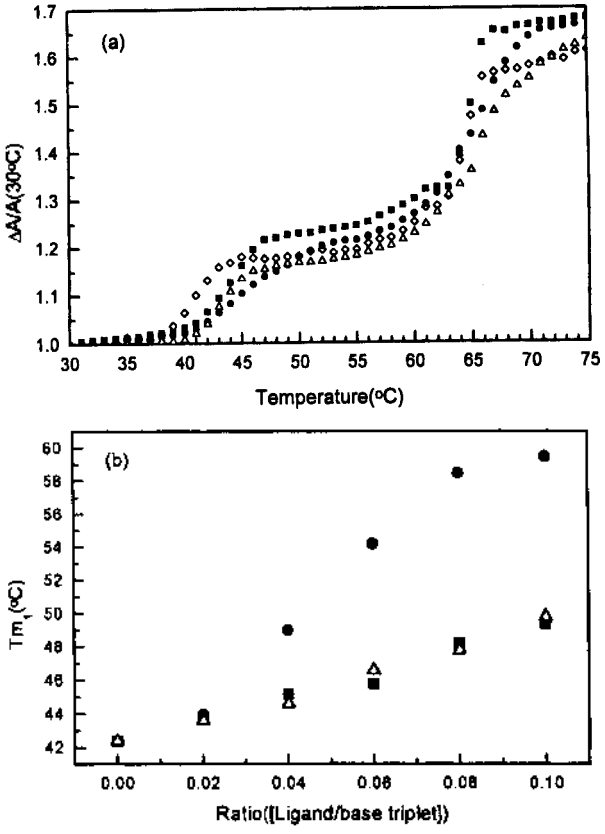

Figure 2. (a) Thermal melting profiles of triple helical poly(dA)·[poly(dT)]$_2$ followed by absorbance change at 260 nm in the absence (◇) and presence of acridine derivatives (■ for 9AA, ● for 9AA-pro, (△ for bis-9AA). The ratios for [ligand]/[base triplet] is 0.02. The concentration of poly(dA)·[poly(dT)]$_2$ triplex is 14 (M in base triplet. (b) Effect of the acridine derivatives on the T_m with the increasing [drug]/[base triplet] ratios.

flavine complexed with triplex poly(dA)·[poly(dT)]$_2$. A difference in the triplex stabilization effect may be caused by difference in the conformation of the binding pocket of the acridine moiety. To clarify this point, the conformation of 9AA-pro and proflavine bound to the poly (dA)·[poly(dT)]$_2$ triplex was compared to those of the 9AA- and bis-9AA-poly(dA)·[poly(dT)]$_2$ complex. The spectroscopic properties of the 9AA- and bis-9AA-poly(dA)·[poly(dT)]$_2$ complexes were thoroughly studied by conventional optical spectroscopy.[32] The triple helical DNA-bound 9AA, as well as bis-9AA were characterized by hypochromism and a red-shift in the acridine absorption band, a positive induced CD spectrum and a strong negative signal in the LD spectrum, as previously reported.[32] All our results indicated that the acridine moiety is intercalated between the base triplets of the poly(dA)·[poly(dT)]$_2$ triplex. In this work, we repeated the same measurements for the 9AA- and bis-9AA-poly(dA)·[poly(dT)]$_2$ complex, and since the results were the same as those previously reported by Kim and his coworkers,[32] we are limiting our discussion to the 9AA-pro and proflavine.

The absorption spectra of free 9AA-pro and that in the presence of a poly(dA)·[poly(dT)]$_2$ triplex are depicted in Figure 3a (the absorption spectrum of the poly(dA)·[poly (dT)]$_2$ triplex is subtracted for easy comparison). The 9AA-pro-triplex complex showed ~40% hypochromism. As previously indicated with 9AA and bis-9AA, the absorption peak in the short wavelength did not shift, but at a longer wavelength a red-shift of ~8 nm was observed for the 9AA complexed with the triplex. The hypochromism, as well as the red-shift in the long wavelength region, was somewhat larger than that observed for 9AA and bis-9AA.[32]

The origin of the induced CD signal for a drug bound to a polynucleotide is very complicated and extremely sensitive to the environment of the bound drug.[39,40] A change in the CD in the DNA absorption region represents either a conformational change of the template DNA or an induced CD of the bound drug. Since the origin of the induced CD in this region is unclear, further analysis into the short wavelength of was suspended. The CD spectra of 9AA and bis-9AA complexed with the poly(dA)·[poly(dT)]$_2$ triplex have been studied.[32] A positive induced CD signal in the long wavelength region (~410 nm) was observed in these complexes and was attributed to a long axis polarized transition. The induced CD spectrum of 9AA-pro, after binding to the triplex, is similar to those observed with 9AA and bis-9AA, consisting of a positive CD signal in the 400 nm region (Figure 3b): this suggests that the conformation of 9AA-pro bound to the triplex is similar to that of 9AA and bis-9AA.

The LD spectra of the 9AA-pro complex is depicted in Figure 3c. The complex exhibited negative signals at all wavelengths, indicating that the transition moments are generally oriented more perpendicular than parallel to the triplex helix axis. The LD^r spectra were determined by dividing the LD by the absorption spectra of the complexes. In order to understand the LD^r spectrum of the complexes, the polarization of the acridine transitions must be assigned to an absorption band. The polarization of the acridine transitions was assigned by stretched film experiments,[44,45] and can be summarized as follows: the 350-450 nm band was a short axis polarized transition; the 340 nm region had a weak long axis polarized transition; at 280 nm the weak transitions of both transition overlap; and at 260 nm there was an intense long axis polarized transition. The magnitude of the negative LD^r signal in the DNA absorption region for the 9AA-pro-poly(dA)·[poly(dT)]$_2$ triplex complex was significantly decreased, compared to that of the drug-free triplex (Figure 3d), indicating that the drugs either increased flexibility, bent it, or contributed a positive LD signal of their own (9AA-pro absorb around 260 nm). The latter possibility may be ruled out because the LD^r was reduced at both 260 and 280 nm. Similar decreases in the LD^r magnitude in the DNA absorption region following the binding of acridine derivatives to the triplex were observed for 9AA and bis-9AA.[32] These decreases are in contrast with those of double stranded DNA. With the duplex, intercalation of a drug causes unwinding, stiffening, and elongation of template duplex, resulting in enhancement of the LD^r magnitude in the DNA absorption region. The LD^r band for 9AA-pro in the 350-450 nm region of the complex had the same magnitude as that of the DNA region, indicating that the short axis polarized transition lie parallel to the triplex bases in the bound complex. Since the LD^r at 260 nm is the same as that at 280 nm, the long axis of the acridine is also parallel to the triplex bases. These observations

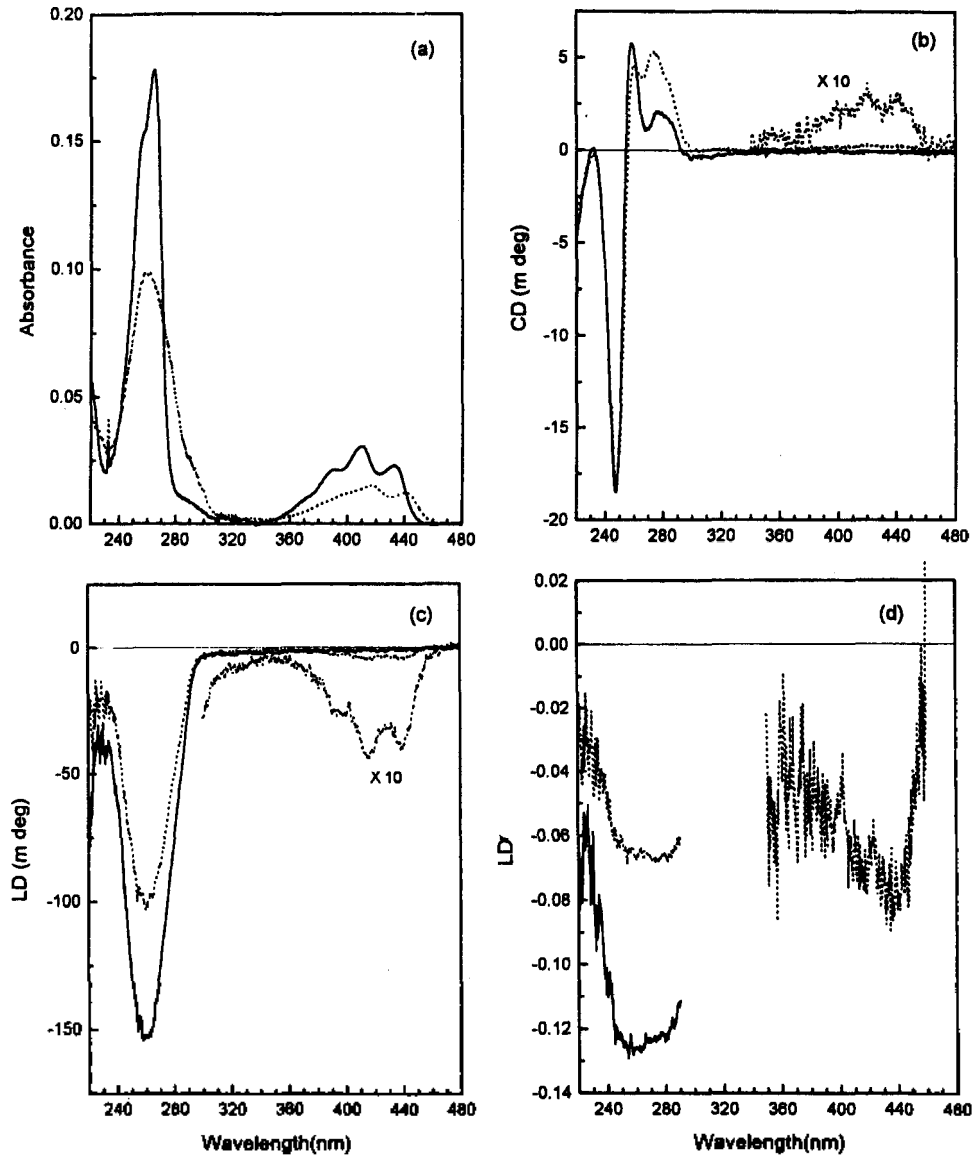

Figure 3. Absorption spectrum(a) and CD(b) of 9AA-pro in the presence (dotted curve) and absence (solid curve) of the poly(dA)·[poly(dT)]$_2$ triplex. Corresponding spectrum of the triplex is subtracted form that of the complex for easy comparison. In (c) and (d), LD and LD' of the drug free triplex (solid curve) and the 9AA-pro-triplex complex (dotted curve) is compared. [9AA-pro]=2.5 μM, [triplex]=25 μM in base triplet.

are indicative of an intercalation binding mode; if the acridine moiety is located in one of the grooves, the angle between the transition moments of the drug and the DNA helix axis is expected to be near 45° thereby resulting in a positive LD' in the drug absorption region.

Proflavine is well known as a DNA intercalator. After binding to the poly(dA)·[poly(dT)]$_2$ triplex, 14.4% hypochromism and 9.5 nm red-shift in the absorption spectrum was observed (Figure 4a), indicating the interaction between the bases of the triplex and proflavine. In contrast to 9AA-pro, the induced CD spectrum in the drug absorption region showed a negative band (Figure 4b). LD characteristics of proflavine complexed with calf thymus DNA and with supercoiled DNA have been previously reported.[46] When it is intercalated to double stranded DNA, the LD' magnitude in the DNA absorption region (258 nm) and drug absorption region (462 nm) are the same, indicating that the transitions of the proflavine are perpendicular to the DNA helix axis. The overall properties of the LD (Figure 4c) and LD' (Figure 4d) spectra of the proflavine-poly(dA)·[poly(dT)]$_2$ complex are the same as those of the proflavine-DNA complex: the magnitude of LD' in the drug absorption region being the same as that of the DNA absorption region. A decrease in the LD' magnitude of the proflavine-poly(dA)·[poly(dT)]$_2$ complex in the DNA absorption region was also apparent, indicating that binding of proflavine to the triplex causes an increase in the flexibility of the poly(dA)·[poly(dT)]$_2$ triplex and/or bent it.

Discussion

Our observations, based on comparative studies of a set of acridine derivatives with poly(dA)·[poly(dT)]$_2$ triplex, are

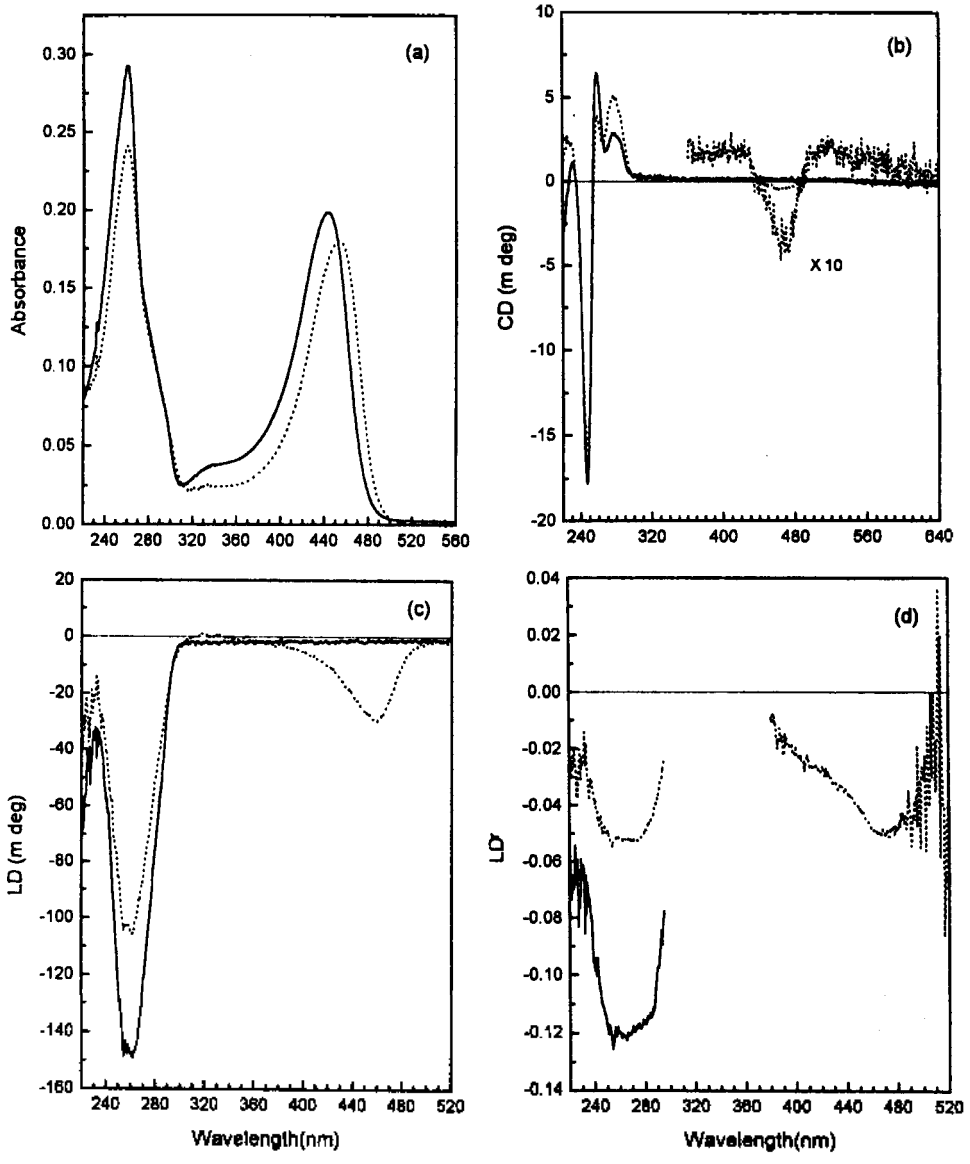

Figure 4. Absorption spectrum(a), CD(b), LD(c) and LD'(d) of proflavine. The conditions and curve assignments are the same as in Figure 3.

summarized as follows:

(1) The binding mode of 9AA-pro to the triplex resembles those of 9AA- and bis-9AA; hypochromism and a red-shift in the absorption spectrum, a weak positive CD signal and a negative LD in the drug absorption region all suggest that the binding modes of 9AA, bis-9AA and 9AA-pro to the poly(dA)·[poly(dT)]$_2$ triplex are similar. In the previous study, the binding modes of 9AA and bis-9AA to poly(dA)·[poly(dT)]$_2$ triplex were similar to the duplex poly(dA)·poly (dT), and poly[d(A-T)$_2$].

(2) The spectroscopic changes in proflavine after binding to poly(dA)·[poly(dT)]$_2$ were similar to those of 9AA, 9AA-pro and bis-9AA, suggesting that the binding mode of proflavine is intercalative in the triplex. The negative CD band in the drug absorption region is attributed to an in-plane rotation of the chromophore by 90° in the intercalation pocket.[39,40]

(3) For all acridines, the magnitude of LD' in the drug absorption region is comparable to that in the DNA absorption region, suggesting that the planar acridine moiety is parallel to the DNA bases of the poly(dA)·[poly(dT)]$_2$ triplex and hence exhibits an intercalative binding mode.

(4) All acridine derivatives caused a significant reduction in the DNA orientation of the triplex in the flow LD experiment, which contrasts with the theory that a simple intercalator significantly increases the degree of orientation of duplex DNA. The reduction in the LD' magnitude may be attributed to a bending or tilt of the triplex near the binding site. Partial denaturation of the helix also causes a reduction in the orientation of the polymer, but this can be ruled out because the melting temperature of the triplex (for both transitions, *i.e.*, triplex to duplex plus single strand and duplex dissociation) in the presence of acridine derivatives increased.

(5) As evidenced by the melting profiles, all acridine derivatives effectively stabilize the Hoogsteen paired third strand. The order of the stabilization effect is 9AA-pro> 9AA>bis-9AA: the effect of 9AA-pro is greater than that of

the other acridine derivatives.

Stabilization of the poly(dA)·[poly(dT)]$_2$ triplex by intercalators. Although it is well known that intercalators stabilize the Hoogsteen paired third strand of the poly(dA)·[poly(dT)]$_2$ triplex,[25~32] the stabilization mechanism is still unclear. The effect of acridine derivatives on the stability of the poly(dA)·[poly(dT)]$_2$ triplex was examined by monitoring the absorbance change at 260 nm. All four drugs stabilized the triplex; 9AA-pro, with an aminoalkyl side chain, was much more effective than the other three acridines. The electrostatic environment of the triplex may change upon drug intercalation, and this may affect the stability of the triplex. In addition, at least two changes in the triplex conformation, possibly related to the triplex stabilization, may occur; (1) the stacking interaction between the intercalator and the DNA base expand to the bases of the third strand, (2) intercalator may be anchored between the bases of the template duplex by stacking, and from there hold the third strand through a hydrogen bond. The first change may be related to the size and shape of the intercalator; molecular modeling studies suggested this for BePI.[28] In the intercalated BePI-poly(dA)·[poly(dT)]$_2$ complex, out of the six DNA bases adjacent to the intercalated BePI, all four Watson-Crick paired bases, and portions of the two bases of the third strand, were within the expanded van der Waals radii of the carbon atoms in the heterocyclic rings of BePI.[28] The second mechanism would result in an elongation of the template duplex while the length of the third strand would remain unchanged; this may explain the decreases observed in the LD' in the DNA absorption region (due to a tilt or bend in the DNA helix axis). For the second mechanism to be in effect, the intercalators must possess a moiety to form the hydrogen bond. Among the acridine derivatives, the amine group may not be a candidate because 9AA, bis-9AA and proflavine (into which the amine group is moved) exhibit the same effect on the third strand stabilization.

The effect of the side chain, which is attached to the intercalator, on stabilizing the triplex has been investigated.[28,31] While ethidium bromide (intercalating moiety plus CH_2CH_3 side chain) and propidium iodide (intercalating moiety plus $(CH_2)_3N^+(CH_2CH_3)_2CH_3$ side chain) effectively stabilize both duplex poly(dA)·poly(dT) and triplex poly(dA)·[poly(dT)]$_2$, ethidium dimer (two ethidium linked by $(CH_2)_3N^+H_2(CH_2)_2N^+H_2(CH_2)_3$ linker) stabilizes only the duplex. However, compared to ethidium, the long side chain of the propidium did not demonstrate any significant additional stabilization for the triplex. The observation that ethidium dimer does not stabilize the third strand of the triplex has been related to the destabilization effect of the side chain: like classical minor groove binding drugs, a linker in the minor groove may have a destabilizing effect on the third strand.[32~36] Energy-minimized models of the BePI-poly(dA)·[poly(dT)]$_2$ and BePI-poly(dA) poly(dT) complexes showed the aminoalkyl chain lying in the major groove of the triplex and in the minor groove of the duplex, with the polycyclic moiety intercalated.[28] The location of the aminoalkyl chain may cause the triplex's selective binding of this class of the molecules and may selectively stabilize the third strand.

We compared the stabilization effect of 9AA, bis-9AA (acridine dimer with aminoalkyl linker), and 9AA-pro (acridine monomer with linker) on a poly(dA)·[poly(dT)]$_2$ triplex. The 9AA-pro stabilized the third strand more effectively than the other acridine derivatives. Bis-9AA was the least effective. As discussed above regarding ethidium dimer, the aminoalkyl side chain, apparently lying in the minor groove, destabilizes the third strand in the bis-9AA case. The number of atoms in the bis-9AA side chain approaches the lower limit for bis-intercalation, and it is probably held tight in the minor groove, resembling a minor groove binding drug. In contrast, the side chain of 9AA-pro lacks the intercalator at one end which anchors the side chain tightly in the minor groove. Therefore, the side chain of 9AA-pro may interact with the negatively charged phosphate group of the DNA stem, reducing the repulsion between the phosphate groups, resulting in an anomalous stabilization effect on the triplex.

Acknowledgment. This work was supported by Korea Research Foundation (Grant No. 01-D-0640).

References

1. LeDoan, T.; Perrouault, L.; Praseuth, D.; Habhoub, N.; Decout, J. L.; Thuong, N. T.; Lhomme, J.; Hélène, C. *Nucleic Acids Res.* **1987**, *15*, 7749.
2. Moser, H. E.; Dervan, P. B. *Science* **1987**, *238*, 645.
3. Lyamichev, V. I.; Mirkin, S. M.; Frank-Kamenetskii, M. D.; Cantor, C. R. *Nucleic Acids Res.* **1988**, *16*, 2165.
4. Mirkin, S. M.; Lyamichev, V. I.; Drushlyak, K. N.; Dobrynin, V. N.; Filipov, A.; Frank-Kamenetskii, M. D. *Nature* **1987**, *330*, 495.
5. Wells, R. D.; Collier, D. A.; Hanvey, J. C.; Shimizu, M.; Wohlrab, F. *FASEB J.* **1988**, *2*, 2939.
6. Htun, H.; Dahlberg, J. E. *Science* **1989**, *243*, 1571.
7. Frank-Kamenetskii *Methods Enzymol.* **1992**, *211*, 180.
8. Thuong, N. T.; Hélène, C. *Angew. Chem. Int. Eng.* **1993**, *32*, 666.
9. Cooney, M.; Czernuszewicz, G.; Postel, E. H.; Flint, S. J.; Hogan, M. E. *Science* **1988**, *241*, 456.
10. Postel, E. H.; Flint, S. J.; Kessler, D. J.; Hogan, M. E. *Proc. Natl. Acad. Sci. USA* **1991**, *88*, 8227.
11. Young, S. L.; Krawczyk, S. H.; Matteucci, M. D.; Toole, J. J. *Proc. Natl. Acad. Sci. USA* **1991**, *88*, 10023.
12. Duval-Valentine, G.; Thuong, N. T.; Hélène, C. *Proc. Natl. Acad. Sci. USA* **1992**, *89*, 504.
13. Grigoriev, M.; Praseuth, D.; Robin, P.; Hemar, A.; Saison-Behmoaras, T.; Dautry-Varsat, A.; Thuong, N. T.; Hélène, C.; Harel-Bellan, A. *J. Biol. Chem.* **1992**, *267*, 3389.
14. Birg, F.; Praseuth, D.; Zerial, A.; Thuong, N. T.; Asseline, U.; LeDoan, T.; Hélène, C. *Nucleic Acids Res.* **1990**, *18*, 2901.
15. Giovannangeli, C.; Thuong, N. T.; Hélène, C. *Proc. Natl. Acad. Sci. USA* **1993**, *90*, 10013.
16. François, J. C.; Saison-Behmoaras, T.; Thuong, N. T.; Hélène, C. *Biochemistry* **1989**, *28*, 9617.
17. Maher, L. J. III.; Wold, B.; Dervan, P. B. *Science* **1989**, *245*, 725.
18. Hanvey, J. C.; Shimizu, M.; Wells, R. D. *Nucleic Acids Res.* **1990**, *18*, 157.
19. Lyamichev, V. I.; Mirkin, S. M.; Frank-Kamenetskii, M.

D. *J. Biomol. Str. Dyn.* **1986**, *3*, 667.
20. Htun, H.; Dahlberg, J. E. *Science* **1988**, *241*, 1791.
21. Johnston, B. H. *Science* **1988**, *241*, 1800.
22. Takasugi, M.; Guendouz, A.; Chassignol, M.; Decout, J. L.; Lhomme, J.; Thuong, N. T.; Hélène, C. *Proc. Natl. Acad. Sci. USA* **1991**, *88*, 5602.
23. Giovannangeli, C.; Thuong, N. T.; Hélène, C. *Proc. Natl. Acad. Sci. USA* **1993**, *90*, 10013.
24. Sun, J. S.; François, J. C.; Montenay-Garestier, T.; Saison-Behmoaras, T.; Roig, V.; Thuong, N. T.; Hélène, C. *Proc. Natl. Acad. Sci. USA* **1989**, *86*, 9198.
25. Mergny, J. L.; Duval-Valentine, G.; Nguyen, C. H.; Perrouault, L.; Faucon, B.; Rougée, M.; Montenay-Garestier, T.; Bisagni, E.; Hélène, C. *Science* **1992**, *256*, 1681.
26. Lee, J. S.; Latimer, L. J. P.; Hampel,, K. J. *Biochemistry* **1993**, *32*, 5591.
27. Pilch, D. S.; Martin, M. T.; Nguyen, C. H.; Sun, J. S.; Bisagni, E.; Montenay-Garestier, T.; Hélène, C. *J. Am. Chem. Soc.* **1993**, *115*, 9942.
28. Pilch, D. S.; Waring, M. J.; Sun, J. S.; Roug, M.; Nguyen, C. H.; Montenay-Garestier, T.; Hélène, C. *J. Mol. Biol.* **1993**, *232*, 926.
29. Wilson, W. D.; Tanious, F. A.; Mizan, S.; Yao, S.; Kiselyov, A. S.; Zon, G., Strekowski, L. *Biochemistry* **1993**, *32*, 10614.
30. Scaria, P. V.; Shafer, R. H. *J. Biol. Chem.* **1991**, *266*, 5417.
31. Tuite, E.; Nordén, B. *Bioorg. Med. Chem.* **1995**, *3*, 701.
32. Kim, H.-K.; Kim, J-M.; Kim, S. K.; Rodgér, A.; Nordé n, B. *Biochemistry* **1996**, *35*, 1187.
33. Howard, F. B.; Todd Miles, H.; Liu, K.; Frazier, J.; Raghunathan, G.; Sasisekharan, V. *Biochemistry* **1992**, *31*, 10671.
34. Umemoto, K.; Sarma, M. H.; Gupta, G.; Luo, J.; Sarma, R. H. *J. Am. Chem. Soc.* **1990**, *112*, 4539.
35. Durand, M.; Thuong, N. T.; Maurizot, J. C. *J. Biol. Chem.* **1992**, *267*, 24394.
36. Durand, M.; Thuong, N. T.; Maurizot, J. C. *J. Biomol. Str. Dyn.* **1994**, *11*, 1191.
37. Kim, S. K.; Nordén, B. *FEBS Lett.* **1993**, *315*, 61.
38. Tuite, E.; Nordén, B. *J. Chem. Soc., Chem. Commun.* **1995b**, 53.
39. Lyng, R.; Rodger, A.; Nordén, B. *Biopolymer* **1991**, *31*, 1709.
40. Lyng, R.; Rodger, A.; Nordén, B. *Biopolymer* **1992**, *32*, 1201.
41. Nordén, B.; Kubista, M.; Kurucsev, T. *Q. Rev. Biophys.* **1992**, *25*, 51.
42. Nordén, B.; Seth, S. *Appl. Spectrosc.* **1985**, *39*, 647.
43. Nordén, B.; Kurucsev, T. *J. Mol. Recognit.* **1994**, *7*, 141.
44. Matsuoka, Y.; Nordén, B. *Chem. Phys. Lett.* **1982**, *85*, 302.
45. Fornasiero, D.; Kurucsev, T. *Chem. Phys. Lett.* **1985**, *117*, 176.
46. Swenberg, C. E.; Carberry, S. E.; Geacintov, N. E. *Biopolymers* **1990**, *29*, 1735.

Synthesis of 4*H*,6*H*-Furo[3,4-c]isoxazole Derivatives as New Potent Fungicides and Their Structure Activity Relationship

Hyung Jin Kim*, Kwang-Jin Hwang†, and Jae Hyun Lee‡

Department of Chemical Technology, Chonnam National University, Kwangju 500-757, Korea
†Department of Industrial Chemistry, Hongik University, Jochiwon 339-800, Korea
‡Korea Research Institute of Chemical Technology, P. O. Box 107, Yusong, Daejeon 305-606, Korea
Received March 5, 1997

4*H*,6*H*-Furo[3,4-*c*]isoxazoles (**I-IV**), potential fungicides, have been designed and synthesized *via* intramolecular [2+3] cycloaddition of nitroalkyne **3** as a key step. The broad spectrum of fungicidal activities of furoisoxazoles (**I-IV**) were observed on plant pathogens at 250 ppm. Furoisoxazoles **II**, **III** with chlorophenyl at 6-position and methyl or alkylated oxime group at 3-position gave effective control of plant diseases. The furoisoxazole **IV** with a chlorophenyl group at 4-position also resulted in high fungicidal activities.

Introduction

In an effort to find a new lead compound as a plant fungicide, we were interested in the isoxazole derivatives. Many isoxazole derivatives show diverse medicinal and agricultural activities such as herbicidal, fungicidal, analgesic, anti-inflammatory, anti-microbial and CNS depression effect.[1-8] After consideration of synthetic aspect, we have designed furo[3,4-*c*]isoxazoles (**I-IV**), in which the fused isoxazole nucleus might provide potential fungicidal activity. Our preliminary research showed that furoisoxazoles **I** with *o*- or *p*-chlorophenyl substituent on 6-position and methyl on 3-position have a broad spectrum of fungicidal activities against representative six plant fungi.[9,10] Based on these results, we have continued further structural derivatization of furoisoxazole **I** to study structure activity relationship and eventually to enhance its fungicidal activity. Here, we report an efficient preparation of novel bicyclic isoxazole derivatives